Trends Pharmacol. Drug Deliv., 2025, 1, Iss. X, 39-56
DOI: 10.62184/tpdd.jtpdd110020243

SCIENCE PARK PUBLISHER
Trends in Pharmacology and Drug Delivery

Research article

A prodigiosin/surfactin nanobiotechnological formulation: Development and characterization

Amira M. Heneidy[1], Dina M. Mahdy[2], Hoda E. Mahmoud[1], Alyaa A. Ramadan[3,*], Ahmed Hussein[1], Maged W. Helmy[4] and Labiba El-Khordagui[3]

[1] *Department of Biotechnology, Institute of Graduate Studies and Research, Alexandria University, Alexandria, Egypt*
[2] *Department of Pharmaceutics, College of Pharmacy, Arab Academy for Science, Technology and Maritime Transport, Alamein, Egypt*
[3] *Department of Pharmaceutics, Faculty of Pharmacy, Alexandria University, Alexandria, Egypt*
[4] *Department of Pharmacology and Toxicology, Faculty of Pharmacy, Damanhour University, Damanhour, Egypt*

Received: 13 November 2024
Revised: 04 March 2025
Accepted: 07 March 2025
Published: 17 April 2025

Keywords:
Prodigiosin, Surfactin, *Serratia marcescens*, Nanomicelles, Anticancer activity

Corresponding author*:
Alyaa A. Ramadan
Email: alyaa.ramadan@alexu.edu.eg

Abstract: There is a growing global interest in developing greener and safer pharmaceutical formulations that minimize environmental impact. In this study, we present a biotechnological nanoformulation combining prodigiosin (PG), a water-insoluble, microbially derived red pigment with multifunctional bioactivity and surfactin (SF), a lipopeptide biosurfactant known for its diverse surface-active properties. PG was produced by *Serratia marcescens*, spectrally characterized, and subsequently incorporated into preformed SF nanomicelles (nSF) via thermal sonication at 50 °C, yielding PG-loaded nanomicelles (nPG/SF). Physicochemical characterization of nPG/SF revealed spherical nanostructures with an average diameter of 227 ± 18.95 nm, a moderate polydispersity index (PDI) of 0.59 ± 0.17, a negative surface charge (-27.1 ± 0.97 mV), high entrapment efficiency (98%), and physical stability at 4 °C for at least 14 days. In terms of bioactivity, nanomicellization appeared to enhance the antibacterial effect of PG against *Staphylococcus aureus* and a clinical isolate of *Pseudomonas aeruginosa*, while significantly ($p < 0.05$) improving SF's cytotoxic activity against two breast cancer cell lines, MCF-7 and MDA-MB-231. Furthermore, using nSF as a carrier slightly increased PG's anticancer activity, suggesting the potential for dose reduction of both PG and SF. Overall, this study provides a proof of concept for an eco-friendly, biosurfactant-based nanomicellar PG formulation with improved solubility, stability, and bioactivity, supporting its potential in pharmaceutical and biotechnological applications. Further investigations are warranted to validate and extend these findings.

1. Introduction

Surface active agents or surfactants have for decades played important roles in various biomedical fields including pharmaceutical and vaccine formulation, drug delivery, dermatology, and the cosmetics personal care industry among others [1]. However, the steadily growing demand for biocompatibility, biodegradability, and sustainability prompted the prioritization of eco-friendly surfactants for diverse applications. In this context, greener microbially derived surfactants known as biosurfactants are foreseen as the next-generation lower ecological impact surfactants. Biosurfactants are classified as glycolipids, lipopeptides, fatty acids, phospholipids, neutral lipids, and polymeric and particulate types exhibiting several advantages over petroleum-derived surfactants. These include greater surface activity, stability, biocompatibility, biodegradability, and bioactivity in addition to lower toxicity [2].

A key property of biosurfactants as surface-active agents is their ability to self-assemble into core–shell nanostructures, featuring an inner hydrophobic core that can effectively encapsulate water-insoluble or labile drugs. This enhances the solubility, stability, and bioactivity of the incorporated compounds, while also enabling controlled release [3-5]. These advantages have driven interest in biosurfactants as eco-friendly alternatives to

synthetic surfactants in pharmaceutical, drug delivery, healthcare, and detergent applications [6; 7]. Moreover, many biosurfactants exhibit intrinsic drug-like activities with potential therapeutic benefits [8-10].

Among lipopeptide biosurfactants, surfactin (SF) has gained significant attention as a multifunctional agent. Structurally, SF consists of a cyclic heptapeptide containing five lipophilic amino acids and two hydrophilic residues—glutamic acid and aspartic acid—linked to a hydrophobic β-hydroxy fatty acid chain (Figure 1A). According to the literature, SF exhibits a wide range of intrinsic bioactivities, including antimicrobial, anti-inflammatory [10; 11], and anticancer effects [12]. It may function not only as a primary anticancer agent [13] but also as a bioactive pharmaceutical excipient that enhances the therapeutic efficacy of co-delivered drugs [14; 15]. Moreover, SF-based self-assembled nanoparticles (NPs) are characterized by high surface activity, biodegradability, and favorable safety profiles, making them promising nanocarriers for intracellular drug delivery. Notably, SF NPs have been explored for enhancing the bioavailability and cytotoxicity of anticancer drugs such as doxorubicin and bleomycin [16; 17]. More recently, modified SF nanomicelles have emerged as a novel platform for targeted drug delivery in cancer therapy [18; 19].

Despite the expanding body of evidence supporting the pharmaceutical applications of SF, further research is needed to fully explore its potential as a bioactive, micelle-forming agent in drug delivery applications. In this study, we investigate the nanomicellar encapsulation capabilities of SF using a hydrophobic, microbially derived bioactive pigment, prodigiosin (PG) (Figure 1B). The pigment is primarily produced by the Gram-negative bacterium *Serratia marcescens* [20] and is distinguished by its pyrrolyl pyrromethene core and deep blood-red coloration. The choice of PG is driven by the growing interest in bacterial pigments as sustainable, naturally derived anticancer agents, which have demonstrated efficacy against various cancer types with minimal or no toxicity to normal cells [21].

Prodigiosin is a fascinating multifunctional bioactive molecule exhibiting antibacterial, anticancer, anti-inflammatory, and antioxidant activities [22; 23]. As an antibacterial agent, PG acts principally by damaging the bacterial cell membrane and suppressing biofilm-derived antimicrobial resistance [24]. On the other hand, mechanisms of PG anticancer activity include mainly induction of cell cycle arrest, mitochondrial-mediated apoptosis, DNA cleavage and immunomodulation of the tumor microenvironment [22; 25]. In addition, PG inhibits the transforming growth factor beta (TGF-β) signaling [26] and regulates cancer metabolism [27]. We have demonstrated earlier the anticancer efficacy of PG against caco-2, breast cancer, and colorectal cancer cells [28-30].

In spite of such auspicious benefits, biomedical applications of PG have been limited by its high hydrophobicity and insolubility in aqueous media, a formulation problem that has been successfully addressed using a drug delivery approach. In this context, polymeric carriers [29; 31], liposomes [32; 33], metal NPs [34; 35], halloysite [36], and more recently probiotics as emerging bio-targeted drug carriers [28; 30] have been reported as a promising approach for PG delivery and bioactivity enhancement.

The present study aimed to combine PG and SF in an innovative sustainable nanobiotechnology-based formulation based on the entrapment of PG into surfactin self-assembled nanomicelles (nSF) forming a PG/SF nanomicellar formulation (nPG/SF) for potential biomedical applications. The study includes the preparation and comprehensive physicochemical and biological characterization of nPG/SF as a potential nanoformulation integrating the distinct properties and functionalities of its PG and nSF components.

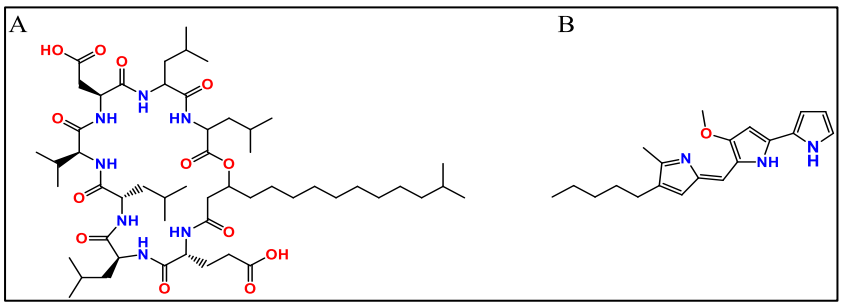

Figure 1. Chemical structure of: (A) Surfactin and (B) prodigiosin.

2. Materials and methods

2.1. Materials

The following materials were used in this study: SurfPro™ surfactin (Lotioncrafter, USA), potassium phosphate monobasic (extra pure, Alpha Chemica, India), yeast extract (Lab M, UK), sodium hydroxide, tryptone, and glacial acetic acid (99.5% extra pure), Loba Chemie Pvt Ltd, India). Hydrochloric acid was obtained from Pioneers for Chemicals (Piochem, Egypt), while petroleum ether (60–80°C) and Tween 80 were sourced from ADWIC, Egypt. Methanol (HPLC grade, 99.8%) was purchased from Fisher Scientific, UK, and ethyl alcohol from the International Company for Supplies & Medical Industries, Egypt. Additionally, ammonium acetate (WINLAB, India), dimethyl sulfoxide (Riedel-de Haën, Germany), Dulbecco's Modified Eagle's Medium (Gibco, Fisher Scientific, UK), and dialysis bags (Visking® 36/32, 24 mm, MWCO12000-14000, Serva, USA) were utilized. All other reagents and chemicals used were of analytical grade. The bacterial strain for prodigiosin biosynthesis, *Serratia marcescens*, was obtained from the culture collection of the Microbial Biotechnology Laboratory, Biotechnology Department, Institute of Graduate Studies and Research, Alexandria University.

2.2. Production and characterization of prodigiosin

The PG red pigment was produced from *Serratia marcescens* (*S. marcescens*) using a peanut powder-based production medium as reported [20]. The pigment was extracted from broth using a petroleum ether and ethanol mixture in a 1:2 (v/v) ratio in a separating funnel. The crude PG precipitate was re-dissolved in 5 mL methanol and the medium was neutralized with 1N HCl. This was followed by complete solid-phase extraction and drying of PG in an oven at 37ºC till almost complete solvent evaporation and the powdered PG was kept at -20ºC protected from light.

2.3. Characterization of prodigiosin

The obtained PG was characterized by ultraviolet-visible (UV-Vis) spectrophotometry, Fourier transform infrared spectroscopy (FTIR), and liquid chromatography-tandem mass spectrometry (LC-MS-MS). The UV-Vis absorption spectrum of a methanolic PG solution was recorded within the wavelength range of 400 to 600 nm against methanol as blank using a single-beam UV-Vis spectrophotometer (Helios Alpha, Germany). A calibration curve was constructed at the determined λ_{max} (538 nm) using a PG methanolic solution of 150-450 µg/mL. The FTIR spectrum of the obtained PG was recorded using the KBr pellet method and a Perkin Elmer FTIR spectrometer, Spectrum BX, USA) within the wavenumber range of 4500-450 cm^{-1}.

For LC-MS-MS analysis, PG was dissolved in methanol and analyzed using HPLC-MS\MS Sciex QTRAP 5500 according to a reported method with slight modification regarding solvent ratio and column size [37]. An Eclipse XDB-C18 reverse phase column (4.6 x 100 mm x 3.5 µm) was used with 0% to 100% linear solvent gradient over 45 min. The eluting solvent consisted of an aqueous phase consisting of distilled water (DW) containing 0.2% acetic acid and an organic phase (methanol / 0.2% acetic acid). PG was detected by electrospray ionization mass spectrometry (ESI-MS). High-resolution ESI-MS spectra were recorded in the m/z range of 50–600 in the positive ion mode [38].

2.4. Preparation of prodigiosin / surfactin nanomicelles

A preliminary study was undertaken to determine the solubility of PG in SF solution. This was achieved by vortex mixing of an excess amount of PG with SF solutions of increasing concentration in deionized water for 10 min at ambient temperature (~25°C) under the exclusion of light followed by equilibration for one hour. The undissolved PG was separated by centrifugation and the solubilized PG was quantified by UV-Vis spectrophotometry at λmax 538 nm, using a linear regression equation.

Based on the solubility data, the prodigiosin/surfactin nanomicelles (nPG/SF) were obtained by a two-step method. Firstly, blank SF nanomicelles (nSF) were formed by sonicating an aqueous SF solution (1mg/ml) for 10 min. The second step involved the incorporation of PG into nSF by sonicating 30 mg of PG with 10 mL of the nSF dispersion for 30 min at 50ºC [39]. Unentrapped PG was separated as insoluble particles by filtration using omit the Whatman filter paper. The filtered nPG/SF dispersion was stored at 4°C pending characterization.

2.5. Characterization of prodigiosin / surfactin nanomicelles

2.5.1. Morphology by transmission electron microscopy (TEM)

The morphology of nPG/SF in comparison with blank nSF was examined by TEM using JSM-1400 PLUS Transmission

Electron Microscope. The dispersions were diluted 30-fold with DW after filtration through Whatman No. 1 filter paper and the diluted samples were sonicated for 5 min. One drop of the dispersion was placed on copper grids and the sample was negatively stained using a 70% uranyl acetate solution for 30s, followed by air drying. The images were captured at 50000x magnification power and 80 kV.

2.5.2. Colloidal properties

The colloidal properties of nPG/SF in comparison with nSF were measured in triplicate using the Malvern Zetasizer Nano ZS90. The ZP measurements were carried out in DW at 25°C, using a cell voltage of 150 V and a current of 5 mA.

2.5.3. Entrapment efficiency

The PG content of nanomicelles was quantified using UV-Vis spectrophotometry. A 100 µL sample of the PG/SF micellar dispersion was dissolved in HPLC-grade methanol. The amount of PG in a 20-fold diluted methanol solution was then determined at λmax 538 nm using a preconstructed calibration curve. The PG entrapment efficiency (EE%) was calculated using the following equation [40]:

$$\mathbf{EE\% = \frac{PG\ content\ (mg)}{Initial\ PG\ amount\ (mg)}\ x\ 100} \quad \mathbf{(1)}$$

2.5.4. Stability study

The chemical stability of PG in nPG/SF was examined at 4°C using a PG methanolic solution (1 mg/mL) as a control. The PG content in the test samples was analyzed by UV-Vis spectrophotometry at λmax 538 nm at different time intervals (0, 1, 2, 3, 4, 5, and 6 days). The physical stability of freshly prepared nPG/SF and nPG/SF stored at 4ºC for 14 days away from light was also examined by digital photography.

2.5.5. Release study

The release of PG from nPG-SF was determined in phosphate buffer saline (PBS, pH 7.4) containing 1% Tween 80 (PBS / 1% Tween 80) using a dialysis method [29]. Presoaked dialysis bags (MWCO12000-14000) were filled with 0.5 mL of nPG-SF dispersion (800 µg/mL) and placed in 5 mL of the release medium. The systems were shaken in a thermostatically controlled shaking water bath at 100 rpm and 37°C. At specified time intervals (0, 1, 6, and 24 h), 1 mL of the release medium was withdrawn, replaced with fresh medium adjusted at 37ºC, and analyzed spectrophotometrically at λmax 535 nm using the release medium as blank. The study was conducted in triplicate. Additionally, change in the release medium color as a result of possible PG release was monitored by digital photography at all sampling times.

2.6. Biological activity studies

These were conducted after obtaining the ethical approval of the Ethics Committee of the Faculty of Pharmacy, Alexandria University, Alexandria, Egypt (AU 06–2022-12-11-3-13).

2.6.1. Hemolytic activity of surfactin (SF)

The in vitro hemolytic activity of SF was assessed using fresh human blood [41]. In brief, a 2 mL-blood sample was obtained from a healthy young female volunteer under medical supervision after obtaining her informed consent and mixed with ethylenediamine tetra-acetic acid (EDTA), then centrifuged at 2500 rpm for 10 min. The resulting red blood cells (RBCs) were washed three times with PBS pH 7.4 and diluted to a 50% suspension using the same buffer. A 50 µL-sample of the RBCs suspension was added to 950 µL of SF solution in DW to achieve final SF concentrations ranging from 5 to 1000 µg/mL. Triton X-100 solutions 0.1% v/v in DW and PBS were used as the positive and negative controls, respectively. All samples were incubated in a shaking water bath at 200 rpm and 37°C for 30 min. Intact erythrocytes were subsequently isolated by centrifugation at 10000 rpm for 5 min and the absorbance (A) of the supernatant was measured at 540 nm. The percentage hemolysis was calculated using the following equation:

$$\mathbf{\%\ Hemolysis} = \frac{\mathbf{A_{Sample} - A_{Negative\ control}}}{\mathbf{A_{Positive\ control} - A_{Negative\ control}}} \times \mathbf{100} \quad \mathbf{(2)}$$

2.6.2. Antibacterial activity of prodigiosin/surfactin nanomicelles (nPG/SF)

The antibacterial activity of nPG/SF dispersion in comparison with its free PG and nSF component as solutions in 10% methanol and DW, respectively was assessed against the Gram- positive *Staphylococcus aureus* (ATCC 29213) and the Gram-negative *Pseudomonas aeruginosa* clinical isolate using the agar well-diffusion method [42]. The concentration of all samples was kept at 2mg/mL. Briefly, 40 mL of melted Luria Bertani-agar medium (tryptone 10 g/ L, yeast extract 5 g/L, NaCl 10 g/L, and agar 20g/L, pH 7.0) was poured after cooling to 55 °C into a sterile Petri dish (9 cm in diameter). After agar solidification, 50 µL of 0.5 McFarland bacterial suspension ($1.5*10^8$ CFU/mL) was spread on the surface of the agar plates

using sterile cotton swabs. Five wells were punched aseptically in the inoculated plates using an inverted sterile blue tip (8 mm in diameter). A 100 µL aliquot of each test sample (PG, SF, and nPG/SF) was added separately to the wells. The fourth and fifth wells were inoculated with 10% methanol as a negative control for free PG. The inoculated plates were incubated statically at 37 °C for 24 h. All treatments were conducted in triplicate.

2.6.3. Cytotoxic activity of prodigiosin/surfactin nanomicelles (nPG/SF)

The cytotoxic activity of nPG/SF in comparison with PG, SF, and nSF at various concentrations was assessed using the human breast adenocarcinoma cell lines MCF-7 and MDA-MB-231. The cells were exposed to the test materials for 48 h at 37°C. The concentration range for PG and nPG/SF was 3.12 - 100 µg/mL while it was 1-40 µg/mL for SF and nSF. Cell viability was assessed in triplicate using DMSO 1% solution as a control and the MTT assay as reported [43]. Absorbance was measured at 570 nm using a microplate reader (Model 550, Bio-Rad, USA). The half-maximal inhibitory concentration (IC_{50}) values were determined using Origin 8.0 software from Origin Lab, Northampton, MA. Dose-response curves were generated after correcting for background absorbance from the controls. The % cell viability was calculated in triplicate relative to the untreated control cells as follows:

$$\% \textbf{ Cell viability} = \frac{\mathbf{A}}{\mathbf{Ac}} \times \mathbf{100} \qquad \textbf{(3)}$$

Where A is the absorbance of treated wells, and Ac is the absorbance of control wells. The median inhibitory concentrations (IC_{50}) were determined using CompuSyn software (CompuSyn, Inc., version 1) according to the Chou-Talalay method [44], which is used to calculate the dose reduction index (DRI).

2.7. Statistical analysis

The mean ± standard deviation (SD) for at least three measurements of colloidal properties, entrapment efficiency, antibacterial activity, and cytotoxicity studies was obtained using Minitab ver. 17 software. The IC_{50} values were determined through non-linear regression analysis of cell viability data. A two-way analysis of variance (ANOVA) was performed using GraphPad Prism 10, followed by Dunnett's test to compare differences across multiple groups. An unpaired t-test was used to estimate the statistical significance of the differences in the antibacterial study. A significance level of $p < 0.05$ was considered indicative of statistical significance.

3. Results and discussion

3.1. Production and characteristics of prodigiosin

The initial yield of crude PG produced by *S. marcescens* using 500 mL of production medium was approximately 1.0 g after liquid-liquid extraction using a separating funnel (Figure 2A). However, the final yield was reduced after further purification via solid-phase extraction followed by drying at 45°C for 2 days in the oven resulting in a final yield of 50 mg. The prepared PG was dissolved in methanol (Figure 2B) and the solution was kept at -20°C away from light for further use.

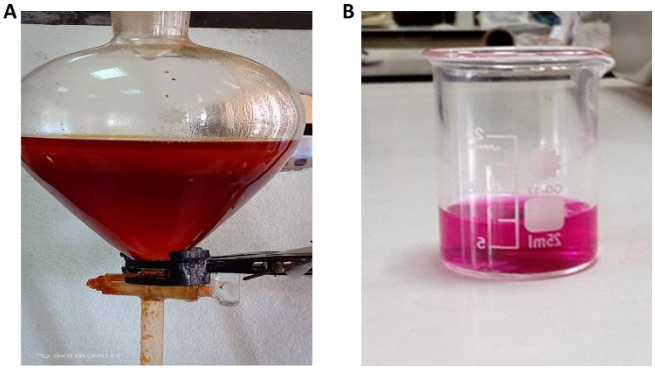

Figure 2. Extraction of prodigiosin produced by *Serratia marcescens*: (A) Liquid-liquid extraction of crude prodigiosin using petroleum ether/ethanol; (B) Purified prodigiosin dissolved in methanol after solid phase extraction.

The prepared PG was characterized by UV-Vis spectrophotometry, FTIR, and LC-MS-MS (Figure 3 A-C). Scanning of a PG methanolic solution in the UV-Vis wavelength range of λ 200 to 800 nm (Figure 3A) revealed a single sharp peak at 538 nm close to the λ_{max} reported for PG [45].

The FTIR spectrum of PG (Figure 3B) showed the fingerprint region of PG characterized by peaks at 1173.4 cm^{-1} and 722.3 cm^{-1} due to the C-O group and C=C group, respectively. A characteristic band at 3393.1 cm^{-1} was assigned to the amine group N-H. Other characteristic bands of the methylene groups appeared at 2922.73 cm^{-1}, 2853.48 cm^{-1}, and 1446.3 cm^{-1}. The C=O peak and the O-H bending peak appeared at 1742 cm^{-1} and 1376.8 cm^{-1}, respectively. In general, the FTIR spectrum of PG was in line with reported spectra [45; 46].

DOI: 10.62184/tpdd.jtpdd110020243

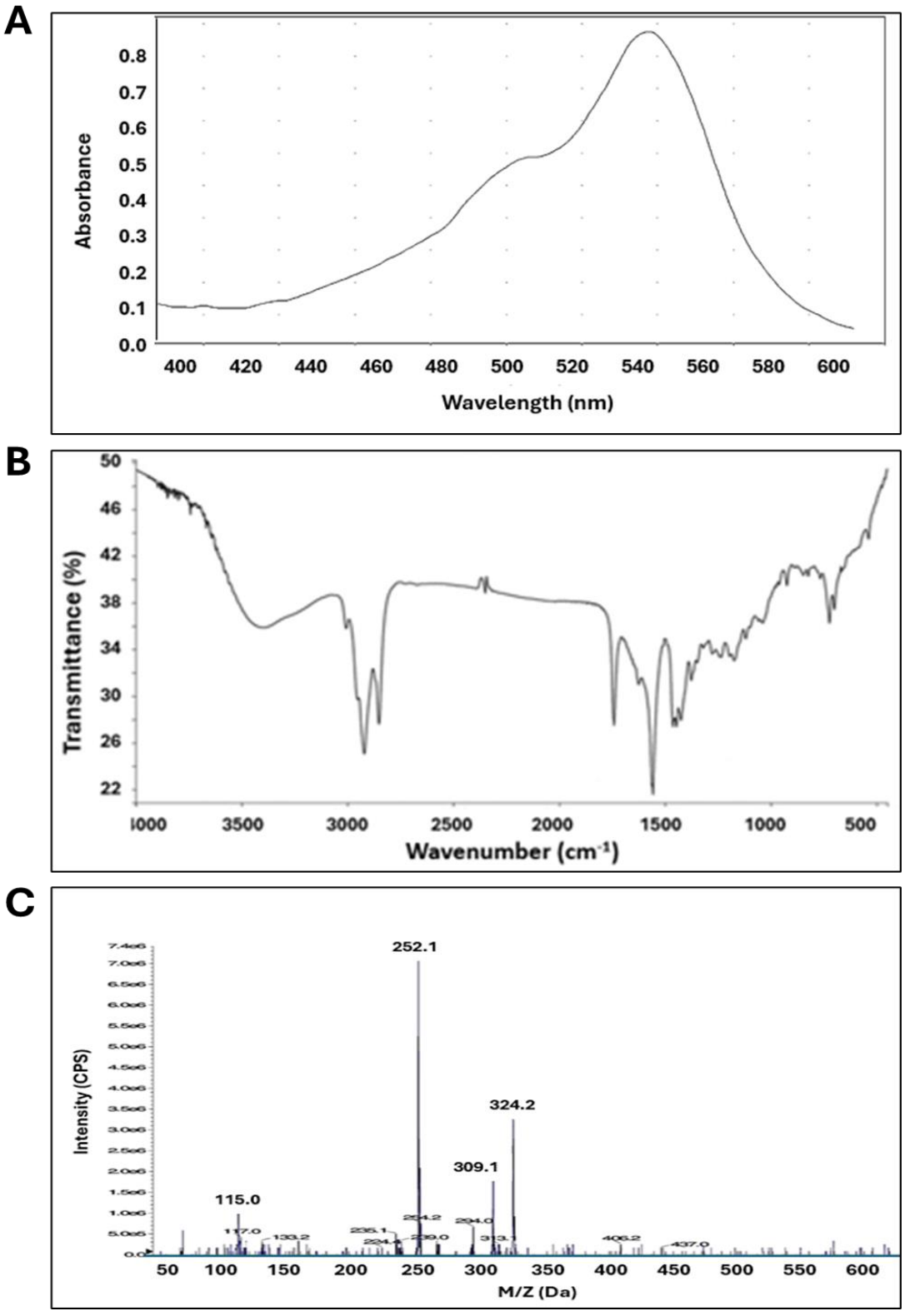

Figure 3. Spectral characteristics of prodigiosin produced by *Serratia marcescens*: (A) UV-Vis spectrum in methanol; (B) FTIR spectrum and (C) LC-MS-MS spectrum.

As shown in Figure 3C, mass spectrometry analysis indicated that the mass-to-charge ratio (m/z) of PG was 324.2 and its MW 324 Da in agreement with reported data [37]. Accordingly, UV-Vis spectrophotometry (λmax 538 nm), the functional groups identified by FTIR analysis and mass spectrometry data verified distinctive characteristics of PG.

3.2. Prodigiosin / surfactin nanomicelles (nPG/SF)

Prodigiosin is known to be insoluble in water. In the present study, PG solubility was increased progressively in SF solutions of increasing concentration up to 2.5 mg/mL in a SF solution of 1mg/mL at ambient temperature (25ºC). This solution concentration exceeded SF critical micelle concentration (CMC) reported to be 21 µg/mL approximately [19], achieving micellar entrapment of PG. Because of its surface activity, SF tends to form nanomicellar structures and larger aggregates in aqueous media [47]. The formation of spherical core-shell micelles with a protruding shell consisting of the two hydrophilic glutamic and aspartic acid residues (Figure 1A) supported by the heptapeptide ring has been documented [48]. Various nanomicellar systems of SF were shown to incorporate hydrophobic drug molecules like itraconazole [4] and ibudilast [5] as well as phospholipids [49]. The aqueous dispersion of PG in SF nanomicelles may provide an alternative to the pigment solution in organic solvents required as a colorant in some applications.

In the present study, nPG/SF was prepared using a two-step method involving the preparation of blank nSF by vortex mixing [50] followed by incorporation of PG in the preformed SF micelles (nSF) by sonication for 30 min at 50ºC. Whatman 0.2 µm filter paper was used to separate undissolved PG to avoid the sorption of PG by membrane filters.

3.3. Characteristics of prodigiosin/surfactin nanomicelles (nPG/SF)

3.3.1. Morphology by transmission electron microscopy (TEM)

As depicted in Figure 4, TEM imaging indicated self-assembly of blank nSF (Figure 4A) and nPG/SF (Figure 4B) in DW into spherical non-aggregated self-assemblies in the nano-size range of 60 to 100 nm.

3.3.2. Colloidal properties

Values for the particle size, polydispersity index (PDI), and zeta potential obtained by DLS for nSF and nPG/SF are shown in Table 1. Data generally indicated favorable colloidal properties. The mean diameter of nSF (172.65 ± 59.25 nm) was not considerably affected by PG loading into the nanomicelles, a common observation reported for hydrophobic drug-loaded nano-self-assemblies where the drug is typically located within their hydrophobic core rather than deposited on the hydrophilic surface [19]. Values for PDI indicated moderate polydispersity in both formulations. Monodispersity is indicated by PDI values below 0.05 while values exceeding 0.7 suggest high polydispersity [51]. It is worth noting that using sonication or heat during nanomicelle formation may lead to a relatively large micelle size distribution [52; 53]. It was observed that the nanomicelle size determined by DLS was larger than that indicated by TEM, a discrepancy attributed to the hydration of nanostructures and the inclusion of agglomerates and aggregates in particle size analysis by DLS [54].

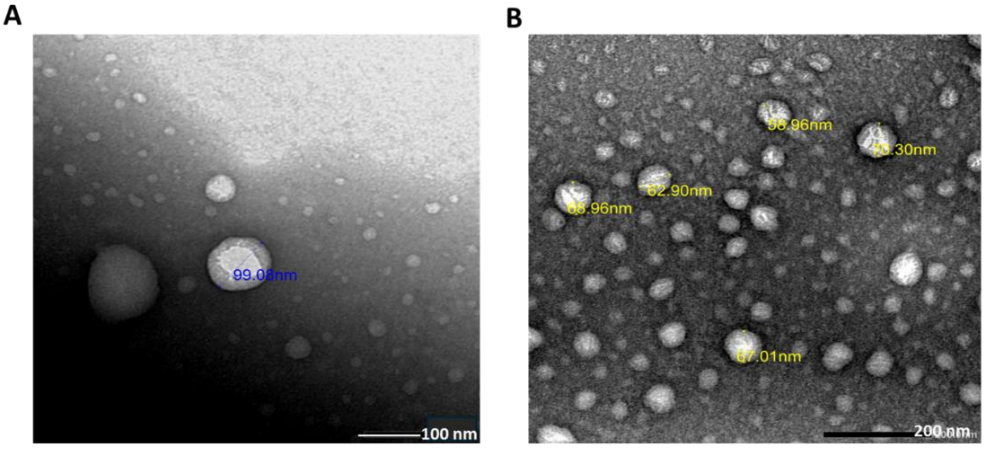

Figure 4. TEM images of (A) Blank surfactin nanomicelles (nSF) and (B) surfactin/prodigiosin nanomicelles (nPG/SF).

Table 1. Colloidal properties of blank surfactin nanomicelles (nSF) and prodigiosin/surfactin nanomicelles (nPG/SF).

Nanomicelles	Particle size, nm	PDI	Zeta potential (ζ), mv
nSF	172.65 ± 59.25	0.65± 0.23	-25.8 ± 1.65
nPG/SF	227.45 ± 18.95	0.59 ± 0.1	-27.1 ± 0.97

According to ζ-zeta potential values, both nSF and nPG/SF displayed a negative surface charge which can be explained by the anionic nature of the SF structure incorporating two acidic amino acids (Figure 1A). The magnitude of ζ-potential values suggests physical stability of the nanomicelles. A ζ-potential of 30 mV is considered sufficient for the effective stabilization of nanodispersions via electrostatic repulsion [55]. Moreover, the incorporation of PG into nSF did not noticeably alter the surface charge as evidenced by the similarity of ζ-potential values, supporting the distribution of PG molecules within the micellar core [56].

3.3.3. Entrapment efficiency (EE%)

Incorporation of PG in a 1 mg/mL dispersion of nSF by sonication at 50ºC for 30 min resulted in 98.33±1.67 % entrapment (Equation 1), verifying micellar solubilization of the pigment. Such a relatively high EE% can be attributed to the ready incorporation of the hydrophobic PG into the hydrophobic core of SF micelles, enhanced by sonication at elevated temperatures. Thermal agitation of surfactant solutions induces the formation of a larger micellar space by surfactants increasing drug incorporation [57]. Additionally, increased solubilization of hydrophobic molecules into SF micelles tends to reduce the micropolarity of the micellar core, promoting further micellar entrapment [58].

3.4. Stability study

Prodigiosin (PG) is known to be sensitive to light and temperature [59] which limits its practical applications. Therefore, this study aimed to evaluate whether encapsulating PG within nSF could enhance its chemical and physical stability under controlled conditions (4 °C, protected from light; Figure 5A–C). As shown in Figure 5A, the chemical stability of free PG, assessed using a methanolic solution as control, showed a marked and progressive degradation, with PG concentration declining to negligible levels by day 6. In contrast, PG encapsulated in nSF retained its chemical integrity throughout the 6-day study period. Assessment of physical stability under the same conditions by digital imaging indicated that the nPG/SF dispersion (Figure 5B) maintained its physical stability with no signs of phase separation for up to 14 days (Figure 5C). Such findings are of importance regarding the storage and use of nPG/SF in different applications.

3.5. Release study

Monitoring of PG release from nPG/SF at 37°C in PBS /1% Tween 80 at 100 rpm by UV-vis spectrophotometry using a dialysis method indicated a lack of PG release as the spectrophotometric absorbance readings of the undiluted samples were negligible over the 24 h-study period. This observation was further supported by digital imaging, which showed no visible coloration in the release medium at any time point, in contrast to the distinct red color of the original nPG/SF dispersion prior to dialysis bag loading (Figure 5D). The absence of PG release is likely attributable to its strong solubilization within the SF nanomicelles and its high hydrophobicity (log $P_{octanol\text{-}water}$ = 5.16), which limits its partitioning into the aqueous release medium under the given conditions. These findings are consistent with previous studies reporting similarly poor PG release from various carrier systems in aqueous environments [28; 30; 60], including PBS with 3% Tween 80 [29].

To summarize, physicochemical characterization data indicated the formation of spherical nPG/SF with a relatively small mean diameter (227 ± 18.95 nm), moderate PDI (0.56 ± 0.1), negative surface charge (-27.1 ± 0.97), and high EE (98% approximately). The nPG/SF can be stored in the refrigerator protected from light for up to 14 days. Accordingly, the nPG/SF nanostructure offers promise as a nanobiotechnological formulation integrating the properties and functionalities of both PG and SF for biomedical applications. This justified undertaking biological activity studies.

DOI: 10.62184/tpdd.jtpdd110020243

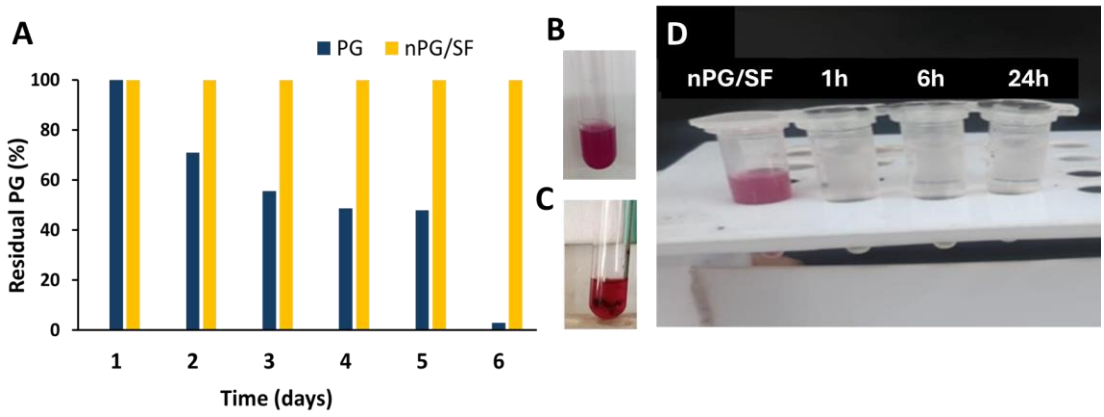

Figure 5. Stability and release properties of nPG/SF nanomicelles. (A) Chemical stability of PG in nSF dispersion in comparison to a methanolic solution at 4ºC protected from light; (B and C) Physical stability of nPG/SF nanomicelles: (B) Freshly prepared and (C) following storage at 4ºC for 14 days protected from light. (D) Digital photographs of the nPG/SF nanomicellar dispersion and samples of the release medium at different time points using a dialysis method and PBS pH 7.4 / 1% Tween 80 as release medium at 37ºC and 100 rpm.

3.6. Biological activity

3.6.1. Hemolytic activity of surfactin

In addition to its exceptional surface activity-related physicochemical properties [6, 61], SF exhibits various bioactivities linked to its amphiphilic nature primarily through interactions with cellular membranes, including those of red blood cells (RBCs) [62]. Given the relevance of SF's hemolytic activity in drug delivery applications—especially those involving systemic administration or direct blood contact—it was essential to identify the concentration range at which SF induces hemolysis. However, as the intense red coloration of PG interferes with hemoglobin absorbance measurements at λmax of 540 nm, hemolytic activity could not be accurately assessed for the nPG/SF formulation, in order to avoid spectral interference and ensure valid results.

The hemolytic activity of SF against human red blood cells (RBCs) was evaluated across a concentration range of 5 to 1000 µg/mL and expressed as percent hemolysis, calculated using Equation 2. Phosphate-buffered saline (PBS) and 0.1% v/v Triton X-100 in distilled water served as negative and positive controls, respectively. As shown in Figure 6A, SF induced concentration-dependent hemolysis, with a noticeable onset at approximately 20 µg/mL, coinciding with its critical micelle concentration (CMC) [19]. In contrast, the negative control induced no hemolysis, while the positive control caused complete (100%) hemolysis (Figure 6B). Visual observations were corroborated by quantitative measurements of hemoglobin release, determined spectrophotometrically at λmax = 540 nm (Figure 6C).

The results showed that SF induced nearly 100% hemolysis at concentrations of 300 µg/mL and above. This pronounced hemolytic activity represents a significant safety concern, particularly for parenteral drug delivery applications. To address this limitation and improve hemocompatibility, various strategies have been explored, including chemical modification of SF to generate linear analogs [62] and structural adjustments aimed at shortening and reducing the hydrophobicity of the β-hydroxy fatty acid chain [61]. Such modifications hold promise for expanding the pharmaceutical and biotechnological utility of SF-based formulations.

3.6.2. Antibacterial activity of prodigiosin/surfactin nanomicelles

The antibacterial activity of the nPG/SF nanoformulation was evaluated in comparison to its individual components, PG and SF, each at a concentration of 2 mg/mL, *against S. aureus* and *P. aeruginosa*. The results, expressed as inhibition zone diameters, are presented in Figure 7. For *S. aureus*, neither the 10% methanol control nor the nSF formulation alone exhibited antibacterial activity at the tested concentration. In contrast, PG in 10% methanol produced a measurable inhibition zone of 1.15 ± 0.0298 cm, confirming its antibacterial effect. Previous studies have attributed PG's antibacterial action to its ability to

DOI: 10.62184/tpdd.jtpdd110020243

disrupt *S. aureus* cell wall and membrane integrity, as well as to inhibit biofilm formation [63]. Notably, the nPG/SF nanoformulation produced a modest but statistically significant increase in the inhibition zone diameter (1.33 ± 0.033 cm; $P < 0.05$), indicating enhanced antibacterial activity relative to PG alone. This improvement may be attributed to the nanomicellar formulation facilitating more effective interactions between the nanocarrier and the bacterial membrane, despite the limited release of PG from the micelles, as demonstrated in Figure 5D

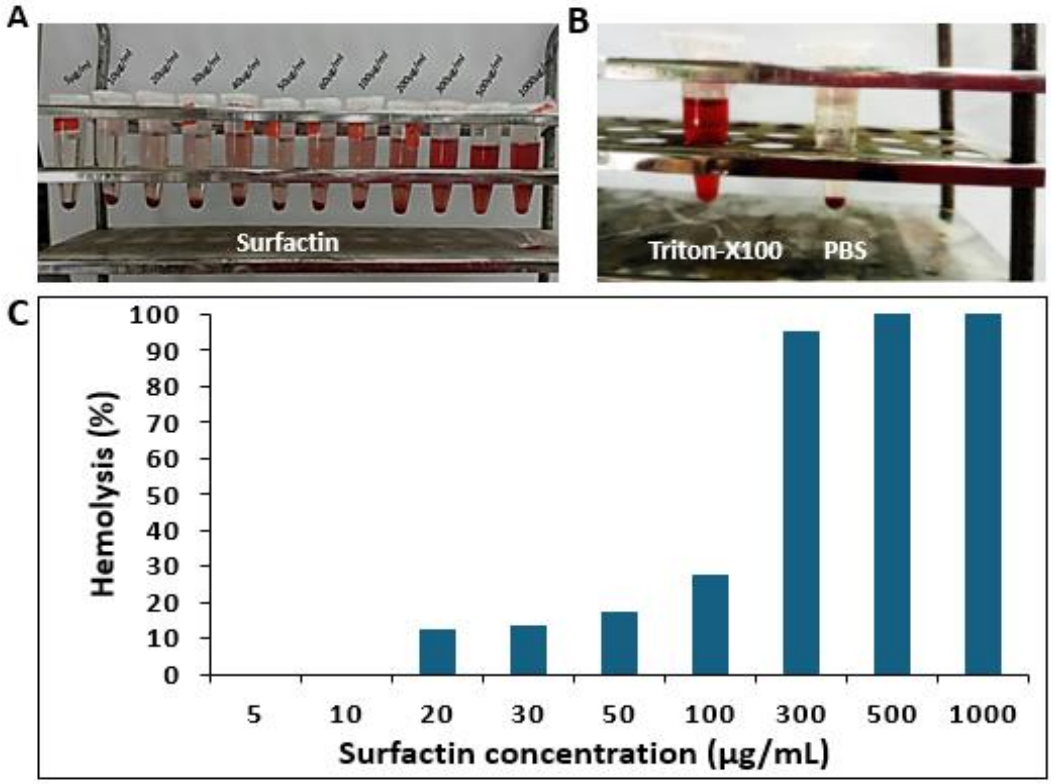

Figure 6. Lysis of human RBCs following incubation with SF in a shaking water bath at 200 rpm and 37°C for 30 min: (A) Induction of hemolysis by surfactin in increasing concentration relative to (B) Triton-X 100 and PBS as positive and negative control, respectively and (C) % hemolysis induced by SF determined by UV-vis spectrophotometry of released hemoglobin at λmax 540 nm.

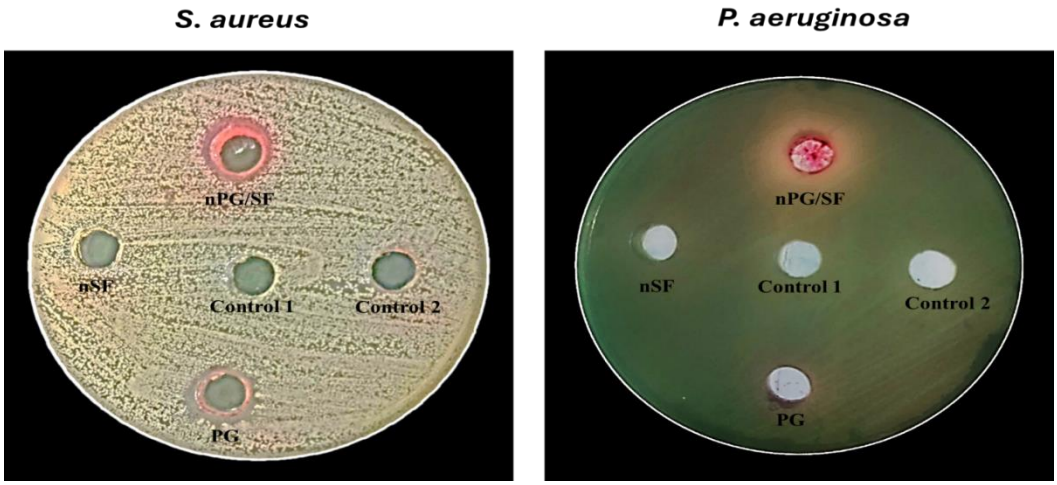

Figure 7. Antibacterial activity of prodigiosin /surfactin nanomicelles (nPG/SF) in comparison with PG solution in 10% methanol and blank surfactin nanomicelles (nSF), all at 2mg/mL concentration against *S. aureus* and *P. aeruginosa* using 10% methanol solution as control and the agar diffusion method.

In the case of the *P. aeruginosa* clinical isolate, no inhibition zones were observed around the wells containing the control or any of the test samples under the study conditions (Figure 7), indicating a lack of direct antibacterial activity at the tested concentration. However, PG appeared to slightly suppress the characteristic green coloration of the culture medium, which results from the synthesis of pyocyanin (blue) and fluorescein (yellow) pigments by *P. aeruginosa* [64]. This pigment-suppressing effect was notably enhanced by the nPG/SF nanoformulation. Given that pyocyanin has been shown to contribute to virulence and the development of antibiotic resistance in *P. aeruginosa* by upregulating various pathogenic factors [65], these findings suggest an alternative mode of action for PG. Previous studies have reported that PG can inhibit bacterial virulence factors such as hemolysins, exotoxins, and proteolytic enzymes without necessarily affecting bacterial viability [66]. The enhanced effect observed with nPG/SF may be due to improved cellular interactions or increased bioavailability of PG in its nanoform, which may allow for more effective suppression of virulence mechanisms. These findings highlight the potential of nPG/SF as a multifunctional antimicrobial formulation capable of impairing bacterial pathogenicity and resistance development, even in the absence of bactericidal activity.

3.6.3. Cytotoxicity of PG/SF nanomicelles and their components

The cytotoxicity of nPG/SF in comparison with its PG and nSF components nanomicelles was assessed using human breast adenocarcinoma MDA-MB-231 (MDA) and MCF-7 cell lines and the MTT assay. These cell lines are well established to model resistant and easier to treat breast cancer, respectively [67]. Data for cytotoxicity (Figure 8) expressed as % cell viability calculated using Equation 3 indicated that all test samples reduced the viability of both MCF-7 and MDA cells to less than 50%.

Cell viability results expressed as IC50 values for MCF-7 and MDA-MB-231 cell lines are listed in Table 2. Statistical analysis was carried out using two-way ANOVA by GraphPad Prism 10 (n=3). It could also be observed that all samples were more active against MCF-7 than MDA cells.

Assessment of cytotoxicity revealed that PG exhibited significantly greater potency than SF ($p < 0.05$), as reflected by lower IC_{50} values against both breast cancer cell lines (Table 2). Both compounds are known for their anticancer properties; however, PG has demonstrated particularly strong cytotoxic effects in both estrogen receptor-positive (MCF-7) and estrogen receptor-negative (MDA-MB-231) breast cancer cells. The mechanisms underlying PG's activity include induction of mitochondrial-dependent apoptosis, characterized by cytochrome c release, activation of caspases-9, -8, and -7, and cleavage of poly (ADP-ribose) polymerase (PARP) [68]. In MCF-7 cells, PG has also been reported to induce genomic instability, evidenced by micronuclei formation [69], and to trigger apoptosis by modulating pro- and anti-apoptotic gene expression [70]. Furthermore, it has been shown to restore the demethylation status and expression of tumor-suppressive miR-200c, contributing to its anticancer efficacy [71]. In the more treatment-resistant MDA-MB-231 cells, PG promotes apoptosis via downregulation of anti-apoptotic B-cell lymphoma 2 (BCL-2) and upregulation of pro-apoptotic BAX and caspase-9 mRNA expression levels [20].

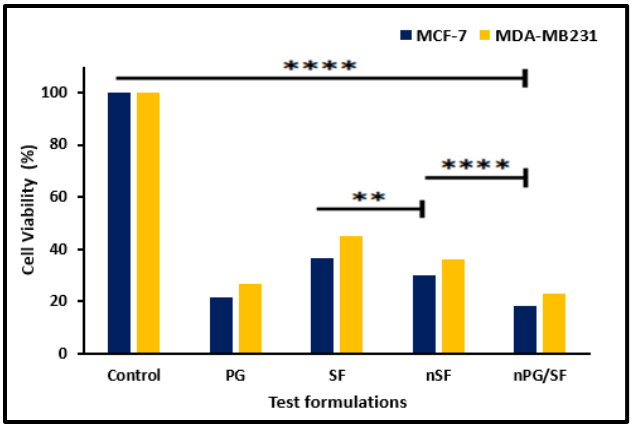

Figure 8. Cell viability data for MCF-7 and MDA-MB 231 cell lines following 48 h exposure to test formulations at 37ºC using the MTT assay and untreated cells as control. Error bars represent SD (n=3). **denotes p=0.0023, and ****denotes p=<0.0001.

Table 2. IC50 values for MCF-7 and MDA-MB-231 cell lines following 48 h cell contact at 37ºC.

Test Formulation	Concentration range, µg/mL	Cell line	
		MCF-7	MDA
		IC_{50} , µg/mL± SD	IC_{50}, µg/mL± SD
PG solution	3.12-100	21.49±1.04	26.96±1.86
SF solution	1.25-40	36.62±2.18	45.13±1.96
nSF	1.25-40	30.02±1.87	36.37±1.56
nPG/SF	3.12-100	18.43±1.78	22.99±1.61

The SF inhibitory effect on breast cancer cells is initiated by a detergent-like effect that disrupts the cell plasma membrane and induces apoptosis, and metastasis [72]. MCF-7 cells were inhibited by SF and its isoforms produced by different Bacillus species in a dose- and time-dependent manner [73]. A more detailed analysis of SF-induced death of MCF-7 cells was related to the generation of reactive oxygen species (ROS) and apoptosis via sustained activation of the phosphorylation of ERK1/2 and JNK signaling pathways [74]. The biosurfactant was reported to inhibit MDA triple-negative breast cancer cells by inducing cell cycle arrest at the G1 phase [75] and suppressing metalloproteinase-9 (MMP-9) expression as well as TPA-induced phosphorylation of Akt and extracellular signal-regulated kinase (ERK) [76].

Interestingly, the cytotoxic activity of SF against both MCF-7 and MDA-MB-231 cell lines was significantly enhanced ($p < 0.0001$) following its self-assembly into nanomicelles, as evidenced by the lower IC_{50} values of nSF compared to the SF solution in DMSO (Table 2). To the best of our knowledge, this observation has not been previously reported. Given that the anticancer activity of biosurfactants is closely associated with their ability to disrupt cellular membranes, it is plausible that the improved cytotoxicity of nSF arises from a more efficient interaction between the nanomicelles and cancer cell membranes, thereby enhancing membrane disruption and promoting cell death. These findings are further supported by recent studies demonstrating increased anticancer efficacy of SF nanomicelles upon conjugation with hyaluronic acid—a targeting ligand known to enhance selective uptake by cancer cells [19]. Collectively, these results underscore the potential of SF nanomicelles as a more potent and efficient platform for cancer therapy.

For the nPG/SF formulation, the incorporation of PG into nSF nanomicelles significantly ($p < 0.05$) enhanced their cytotoxicity. However, the enhancement of PG's cytotoxic effects by nSF was less pronounced under the study conditions, particularly in terms of the concentration range (3.12–100 µg/mL) and exposure time (48 h). Cytotoxicity data revealed that PG slightly increased the cytotoxicity of nSF against MCF-7 and MDA-MB-231 cells by 11.59% and 13.38%, respectively (Table 2), although these differences did not reach statistical significance ($p > 0.05$), as shown in Figure 8. Notably, the cytotoxicity of nPG/SF was significantly greater ($p < 0.0001$) than that of nSF alone after 48 h of exposure. This enhancement in cytotoxicity can be attributed to the increased disruption of cancer cell membranes via the interaction between the nSF nanomicelles and the cell membrane [77-79]. Additionally, a possible synergistic effect between PG and nSF may further contribute to the observed enhanced activity against breast cancer cell lines.

The observed increase in cytotoxicity of nPG/SF compared to nSF enabled a reduction in the required dosages of both PG and nSF, as confirmed by the dose reduction index (DRI). This parameter serves to indicate potential synergy between the two bioactive agents and the degree to which the dosage of each agent can be reduced when combined, relative to their individual dosages [15]. Based on the DRI values calculated from the combined cytotoxic effects of nPG/SF, PG, and nSF at the 50% cell death point for both MCF-7 and MDA-MB-231 cell lines (Table 3), it was found that the dosages of PG and nSF could be

reduced upon their combination into nPG/SF. This is evidenced by the corresponding fold increase in DRI, which is particularly significant in terms of enhancing the safety profile of the formulation.

The main outcomes of the cytotoxicity study include the potential of SF to enhance the anticancer activity of the nPG/SF formulation, allowing for dose reduction of both PG and SF components and the significant enhancement of SF cytotoxicity by self-assembly into nanomicelles.

Table 3. Dose reduction index (DRI) for PG and nSF was determined at 50% death point of MCF-7 and MDA-MB-231 cell lines following 48 h cell exposure at 37ºC.

Cell line	Dose reduction index (DRI)	
	PG	nSF
MCF-7	1.16	7.74
MDA	1.17	7.51

4. Conclusion

A novel nanobiotechnology-based pharmaceutical formulation of prodigiosin and surfactin (nPG/SF) was developed and characterized. This nanoformulation enhanced the physical properties of PG, particularly its solubility and stability, and showed promise in boosting its antibacterial and anticancer activities. The nPG/SF formulation offers a versatile platform for combining biosurfactants and bioactive microbial secondary metabolites, with modulated properties and biofunctionalities, thereby expanding its potential for a wide range of biotechnological and biomedical applications.

Declaration of interest statement

The authors declare that this work has not been done or published before and has no competing interests of any type.

Acknowledgment

The authors wish to thank Prof. Amira Embaby, Department of Biotechnology and Dr Lamiaa Abdel-Rahman, Department of Materials Science, Institute of Graduate Studies and Research, Alexandria University, for their kind support.

Author contributions

Labiba El-Khordagui, Maged Helmy, Alyaa Ramadan and Ahmed Hussein contributed to conceptualization. Amira Heneidy, Dina Mahdy, and Hoda Mahmoud contributed to methodology, data analysis and drafting of manuscript. Labiba El-Khordagui, Maged Helmy and Alyaa Ramadan contributed to manuscript editing.

Author Information

Corresponding Author: Alyaa A. Ramadan*

Email: alyaa.ramadan@alexu.edu.eg

ORCID iD: 0000-0003-2143-7909

Authors' ORCID iD:

Amira M. Heneidy 0009-0006-3524-3194

Dina M. Mahdy 0009-0005-6846-2767

Hoda E. Mahmoud 0000-0003-4726-3281

Ahmed Hussein 0000-0002-6887-2927

Maged W. Helmy 0000-0003-0375-6762

Labiba El-Khordagui 0000-0002-6607-8113

References

[1] Das, B., Kumar, B., Begum, W., Bhattarai, A., Mondal, M. H., & Saha, B. (2022). Comprehensive review on applications of surfactants in vaccine formulation, therapeutic and cosmetic pharmacy and prevention of pulmonary failure due to covid-19. Chemistry Africa, 5(3), 459. https://doi.org/10.1007/s42250-022-00345-0

[2] Fernandes, N. A. T., Simões, L. A., & Dias, D. R. (2023). Comparison of biodegradability, and toxicity effect of biosurfactants with synthetic surfactants, 117-136.. https://doi.org/10.1007/978-3-031-21682-4_6

[3] Shan, M., Meng, F., Tang, C., Zhou, L., Lu, Z., & Lu, Y. (2022). Surfactin effectively improves bioavailability of curcumin by formation of nano-capsulation. Colloids and Surfaces B: Biointerfaces, 215, 112521. https://doi.org/10.1016/j.colsurfb.2022.112521

[4] Usman, F., Farooq, M., Wani, T. A., Ahmad, H., Javed, I., Iqbal, M., Sheikh, F. A., Siddique, F., Zargar, S., & Sheikh, S. (2023). Itraconazole loaded biosurfactin micelles with enhanced antifungal activity: fabrication, evaluation and molecular simulation. Antibiotics, 12(10). https://doi.org/10.3390/antibiotics12101550

[5] sharifian, A., Varshosaz, J., Aliomrani, M., & Kazemi, M. (2024). Polydopamine coated surfactin micelles for brain delivery of ibudilast in multiple sclerosis: Design, optimization, in vitro and in vivo evaluation. Journal of Drug Delivery Science and Technology, 95, 105530. https://doi.org/10.1016/j.jddst.2024.105530

[6] El-Khordagui, L., Badawey, S. E., & Heikal, L. A. (2021). Application of biosurfactants in the production of personal care products, and household detergents and industrial and institutional cleaners. 49-96. https://doi.org/10.1016/B978-0-12-823380-1.00005-8

[7] Karnwal, A., Shrivastava, S., Al-Tawaha, A., Kumar, G., Singh, R., Kumar, A., Mohan, A., Yogita, & Malik, T. (2023). Microbial biosurfactant as an alternate to chemical surfactants for application in cosmetics industries in personal and skin care products: A critical review. Biomed Research International, 2375223. https://doi.org/10.1155/2023/2375223

[8] Puyol McKenna, P., Naughton, P. J., Dooley, J. S. G., Ternan, N. G., Lemoine, P., & Banat, I. M. (2024). Microbial biosurfactants: antimicrobial activity and potential biomedical and therapeutic exploits. Pharmaceuticals (Basel), 17(1). https://doi.org/10.3390/ph17010138

[9] Ukaegbu, C. I., Shah, S. R., Alara, R. O., & Thonda, O. A. (2023). Biosurfactants as potential antitumor agents. 439-460 . https://doi.org/10.1007/978-3-031-21682-4_20

[10] Chen, X., Zhao, H., Lu, Y., Liu, H., Meng, F., Lu, Z., & Lu, Y. (2022). Surfactin mitigates a high-fat diet and streptozotocin-induced type 2 diabetes through improving pancreatic dysfunction and inhibiting inflammatory response. International Journal of Molecular Sciences, 23(19). https://doi.org/10.3390/ijms231911086

[11] Johnson, A., Kong, F., Miao, S., Thomas, S., Ansar, S., & Kong, Z. L. (2021). In-vitro antibacterial and anti-inflammatory effects of surfactin-loaded nanoparticles for periodontitis treatment. Nanomaterials (Basel), 11(2). https://doi.org/10.3390/nano11020356

[12] Walvekar, S., Yasaswi, S., Shetty, K., & Yadav, K. S. (2022). Applications of surfactin and other biosurfactants in anticancer activity, 223-234.. https://doi.org/10.1016/B978-0-323-85146-6.00024-3

[13] Tank, J. G., & Pandya, R. V. (2022). Anti-proliferative activity of surfactins on human cancer cells and their potential use in therapeutics. Peptides, 155, 170836. https://doi.org/10.1016/j.peptides.2022.170836

[14] Thakur, S., Singh, A., Sharma, R., Aurora, R., & Jain, S. K. (2020). Biosurfactants as a novel additive in pharmaceutical formulations: current trends and future implications. Current drug metabolism, 21(11), 885. https://doi.org/10.2174/1389200221666201008143238

[15] El-Sheridy, N. A., El-Moslemany, R. M., Ramadan, A. A., Helmy, M. W., & El-Khordagui, L. K. (2022). Itraconazole for topical treatment of skin carcinogenesis: efficacy enhancement by lipid nanocapsule formulations. Journal of Biomedical Nanotechnology, 18(1), 97. https://doi.org/10.1166/jbn.2022.3217

[16] Huang, W., Lang, Y., Hakeem, A., Lei, Y., Gan, L., & Yang, X. (2018). Surfactin-based nanoparticles loaded with doxorubicin to overcome multidrug resistance in cancers. International Journal of Nanomedicine, 13, 1723. https://doi.org/10.2147/ijn.S157368

[17] Xiong, Y., Kong, J., Yi, S., Feng, X., Duan, Y., & Zhu, X. (2020). Surfactin ameliorated the internalization and inhibitory performances of bleomycin family compounds in tumor cells. Molecular Pharmaceutics Journal, 17(6), 2125. https://doi.org/10.1021/acs.molpharmaceut.0c00281

[18] Bhattacharya, S., Kumar, D., Prajapati, B. G., & Anjum, M. M. (2024). Biosurfactant nanomicelles and peptide integration: novel approaches to targeted gene delivery in colon cancer treatment. Current Medicinal Chemistry, 39177136. https://doi.org/10.2174/0109298673312968240803104252

[19] Badawey, S. E., Heikal, L., Teleb, M., Abu-Serie, M., Bakr, B. A., Khattab, S. N., & El-Khordagui, L. (2024). Biosurfactant-amphiphilized hyaluronic acid: A dual self-assembly anticancer nanoconjugate and drug vector for synergistic chemotherapy. International Journal of

Biological Macromolecules, 271, 132545. https://doi.org/10.1016/j.ijbiomac.2024.132545

[20] Anwar, M. M., Shalaby, M., Embaby, A. M., Saeed, H., Agwa, M. M., & Hussein, A. (2020). Prodigiosin/PU-H71 as a novel potential combined therapy for triple negative breast cancer (TNBC): preclinical insights. Scientific Reports, 10(1), 14706. https://doi.org/10.1038/s41598-020-71157-w

[21] Devi, M., Ramakrishnan, E., Deka, S., & Parasar, D. P. (2024). Bacteria as a source of biopigments and their potential applications. Journal of Microbiological Methods, 106907. https://doi.org/10.1016/j.mimet.2024.106907

[22] Srilekha, V., Krishna, G., Sreelatha, B., Jagadeesh Kumar, E., & Rajeshwari, K. V. N. (2024). Prodigiosin: a fascinating and the most versatile bioactive pigment with diverse applications. Systems Microbiology and Biomanufacturing, 4(1), 66. https://doi.org/10.1007/s43393-023-00192-1

[23] Lu, Y., Liu, D., Jiang, R., Li, Z., & Gao, X. (2024). Prodigiosin: unveiling the crimson wonder - a comprehensive journey from diverse bioactivity to synthesis and yield enhancement. Frontiers in Microbiology 15, 1412776. https://doi.org/10.3389/fmicb.2024.1412776

[24] Ma, Z., Xiao, H., Li, H., Lu, X., Yan, J., Nie, H., & Yin, Q. (2024). Prodigiosin as an antibiofilm agent against the bacterial biofilm-associated infection of *pseudomonas aeruginosa*. Pathogens, 13(2). https://doi.org/10.3390/pathogens13020145

[25] Anwar, M. M., Albanese, C., Hamdy, N. M., & Sultan, A. S. (2022). Rise of the natural red pigment 'prodigiosin' as an immunomodulator in cancer. Cancer Cell International, 22(1), 419. https://doi.org/10.1186/s12935-022-02815-4

[26] Tai, S. B., Huang, C. Y., Chung, C. L., Sung, P. J., Wen, Z. H., & Chen, C. L. (2024). Prodigiosin inhibits transforming growth factor beta signaling by interfering receptor recycling and subcellular translocation in epithelial cells. Molecular Pharmacology, 105(4), 286. https://doi.org/10.1124/molpharm.123.000776

[27] Yang, H. A., Han, T. H., Haam, K., Lee, K. S., Kim, J., Han, T. S., Lee, M. S., & Ban, H. S. (2024). Prodigiosin regulates cancer metabolism through interaction with GLUT1. Natural Product Research, 1. https://doi.org/10.1080/14786419.2024.2367241

[28] Abdullah, N. A., Mahmoud, H. E., El-Nikhely, N. A., Hussein, A. A., & El-Khordagui, L. K. (2023). Carbon dots labeled Lactiplantibacillus plantarum: a fluorescent multifunctional biocarrier for anticancer drug delivery. Frontiers in Bioengineering and Biotechnology, 11, 1166094. https://doi.org/10.3389/fbioe.2023.1166094

[29] Mohamed, W. A., El-Nekhily, N. A., Mahmoud, H. E., Hussein, A. A., & Sabra, S. A. (2024). Prodigiosin/celecoxib-loaded into zein/sodium caseinate nanoparticles as a potential therapy for triple negative breast cancer. Scientific Reports, 14(1), 181. https://doi.org/10.1038/s41598-023-50531-4

[30] Saleh, N., Mahmoud, H. E., Eltaher, H., Helmy, M., El-Khordagui, L., & Hussein, A. A. (2023). Prodigiosin-functionalized probiotic ghosts as a bioinspired combination against colorectal cancer cells. Probiotics and Antimicrobial Proteins, 15(5), 1271. https://doi.org/10.1007/s12602-022-09980-y

[31] Majumdar, S., Mandal, T., & Mandal, D. D. (2022). Chitosan based micro and nano-particulate delivery systems for bacterial prodigiosin: Optimization and toxicity in animal model system. International Journal of Biological Macromolecules, 222, 2966. https://doi.org/10.1016/j.ijbiomac.2022.10.072

[32] Rashidi, M., & Jebali, A. (2019). Liposomal prodigiosin and plasmid encoding serial GCA nucleotides reduce inflammation in microglial and astrocyte cells by ATM/ATR signaling. Journal of Neuroimmunology, 326, 75. https://doi.org/10.1016/j.jneuroim.2018.11.014

[33] Valença, A. S. C., Barbosa, A. T. A., Dolabella, S. S., Severino, P., Matos, C., Krambeck, K., Souto, B. E., & Jain, S. (2023). Antimicrobial bacterial metabolites: properties, applications and loading in liposomes for site-specific delivery. Current Pharmaceutical Design, 29(28), 2191. http://dx.doi.org/10.2174/1381612829666230918111014

[34] El-Batal, A. I., El-Hendawy, H. H., & Faraag, A. H. (2017). In silico and in vitro cytotoxic effect of prodigiosin-conjugated silver nanoparticles on liver cancer cells (HepG2). BioTechnologia. Journal of Biotechnology Computational Biology and Bionanotechnology, 98(3). https://doi.org/10.5114/bta.2017.70801

[35] Kassab, R. B., Elbaz, M., Oyouni, A. A. A., Mufti, A. H., Theyab, A., Al-Brakati, A., Mohamed, H. A., Hebishy, A.

M. S., Elmallah, M. I. Y., Abdelfattah, M. S., & Abdel Moneim, A. E. (2022). Anticolitic activity of prodigiosin loaded with selenium nanoparticles on acetic acid–induced colitis in rats. Environmental Science and Pollution Research, 29(37), 55790. https://doi.org/10.1007/s11356-022-19747-1

[36] Guryanov, I., Naumenko, E., Akhatova, F., Lazzara, G., Cavallaro, G., Nigamatzyanova, L., & Fakhrullin, R. (2020). Selective cytotoxic activity of prodigiosin@halloysite nanoformulation [original research]. Frontiers in Bioengineering and Biotechnology, 8. https://doi.org/10.3389/fbioe.2020.00424

[37] Hage-Hülsmann, J., Grünberger, A., Thies, S., Santiago-Schübel, B., Klein, A. S., Pietruszka, J., Binder, D., Hilgers, F., Domröse, A., Drepper, T., Kohlheyer, D., Jaeger, K.-E., & Loeschcke, A. (2018). Natural biocide cocktails: combinatorial antibiotic effects of prodigiosin and biosurfactants. PLOS ONE, 13(7), e0200940. https://doi.org/10.1371/journal.pone.0200940

[38] Lee, J. S., Kim, Y.-S., Park, S., Kim, J., Kang, S.-J., Lee, M.-H., Ryu, S., Choi, J. M., Oh, T.-K., & Yoon, J.-H. (2011). Exceptional production of both prodigiosin and cycloprodigiosin as major metabolic constituents by a novel marine bacterium, Zooshikella rubidus S1-1. Applied and Environmental Microbiology, 77(14), 4967. https://doi.org/10.1128/AEM.01986-10

[39] Taurozzi, J., Hackley, V., & Wiesner, M. (2012). Preparation of nanoparticle dispersions from powdered material using ultrasonic disruption. NIST Special Publication 1200-2. NIST Special Publication, 1200,2. https://doi.org/10.6028/NIST.SP.1200-2

[40] Jangid, A. K., Patel, K., Jain, P., Patel, S., Gupta, N., Pooja, D., & Kulhari, H. (2020). Inulin-pluronic-stearic acid based double folded nanomicelles for pH-responsive delivery of resveratrol. Carbohydrate Polymers, 247, 116730. https://doi.org/10.1016/j.carbpol.2020.116730

[41] Eissa, M. M., El-Moslemany, R. M., Ramadan, A. A., Amer, E. I., El-Azzouni, M. Z., & El-Khordagui, L. K. (2015). Miltefosine lipid nanocapsules for single dose oral treatment of schistosomiasis mansoni: A preclinical study. PLOS ONE, 10(11), e0141788. https://doi.org/10.1371/journal.pone.0141788

[42] Mohamed, S. A., Mahmoud, H. E., Embaby, A. M., Haroun, M., & Sabra, S. A. (2024). Lactoferrin/pectin nanocomplex encapsulating ciprofloxacin and naringin as a lung targeting antibacterial nanoplatform with oxidative stress alleviating effect. International Journal of Biological Macromolecules, 261(Pt 2), 129842. https://doi.org/10.1016/j.ijbiomac.2024.129842

[43] Helmy, M., Ghoneim, A. I., Katary, M. A., & Elmahdy, R. K. (2020). The synergistic anti-proliferative effect of the combination of diosmin and BEZ-235 (dactolisib) on the HCT-116 colorectal cancer cell line occurs through inhibition of the PI3K/Akt/mTOR/NF-κB axis. Molecular Biology Reports, 47(3), 2217. https://doi.org/10.1007/s11033-020-05327-4

[44] Chou, T. C. (2010). Drug combination studies and their synergy quantification using the Chou-Talalay method. Cancer Research, 70(2), 440. https://doi.org/10.1158/0008-5472.Can-09-1947

[45] Arivizhivendhan, K. V., Boopathy, R., Maharaja, P., Regina Mary, R., & Sekaran, G. (2015). Bioactive prodigiosin-impregnated cellulose matrix for the removal of pathogenic bacteria from aqueous solution [https://doi.org/10.1039/C5RA09172A]. RSC Advances, 5(84), 68621. 10.1039/C5RA09172A

[46] Mousavi, S. M., Archangi, B., Zolgharnein, H., & Zamani, I. (2021). Biocolorant “prodigiosin” interferes with the growth of biofouling bacteria: an in vitro and in silico approach. Pigment & Resin Technology. http://dx.doi.org/10.1108/PRT-07-2020-0079

[47] Bochynek, M., Lewinska, A., Witwicki, M., Debczak, A., & Lukaszewicz, M. (2023). Formation and structural features of micelles formed by surfactin homologues. Frontiers in Bioengineering and Biotechnology, 11, 1211319. https://doi.org/10.3389/fbioe.2023.1211319

[48] Shen, H.-H., Thomas, R. K., Chen, C.-Y., Darton, R. C., Baker, S. C., & Penfold, J. (2009). Aggregation of the naturally occurring lipopeptide, surfactin, at interfaces and in solution: an unusual type of surfactant? Langmuir, 25(7), 4211. https://doi.org/10.1021/la802913x

[49] Imura, T., Yanagisawa, S., Ikeda, Y., Moriyama, R., Sakai, K., Sakai, H., & Taira, T. (2024). Solubilization of phospholipid by surfactin leading to lipid nanodisc and

fibrous architecture formation. Molecules, 29(6). https://doi.org/10.3390/molecules29061300

[50] Modabber, G., Akhavan Sepahi, A., Yazdian, F., & Rashedi, H. (2023). Evaluation of production of lipopeptide biosurfactants and surfactin micelles by native Bacillus of Iran, for a broader application range. Journal of Surfactants and Detergents, 26(1), 3. https://doi.org/10.1002/jsde.12626

[51] Masarudin, M. J., Cutts, S. M., Evison, B. J., Phillips, D. R., & Pigram, P. J. (2015). Factors determining the stability, size distribution, and cellular accumulation of small, monodisperse chitosan nanoparticles as candidate vectors for anticancer drug delivery: application to the passive encapsulation of [(14)C]-doxorubicin. Nanotechnology, Science and Applications, 8, 67. https://doi.org/10.2147/nsa.S91785

[52] Alopaeus, J. F., Hagesæther, E., & Tho, I. (2019). Micellisation mechanism and behaviour of Soluplus®–furosemide micelles: Preformulation studies of an oral nanocarrier-based system. Pharmaceuticals, 12(1), 15. https://doi.org/10.3390/ph12010015

[53] Li, J., Huo, M., Wang, J., Zhou, J., Mohammad, J. M., Zhang, Y., Zhu, Q., Waddad, A. Y., & Zhang, Q. (2012). Redox-sensitive micelles self-assembled from amphiphilic hyaluronic acid-deoxycholic acid conjugates for targeted intracellular delivery of paclitaxel. Biomaterials, 33(7), 2310-2320. https://doi.org/10.1016/j.biomaterials.2011.11.022

[54] Souza, T. G., Ciminelli, V. S., & Mohallem, N. D. S. (2016). A comparison of TEM and DLS methods to characterize size distribution of ceramic nanoparticles. Journal of Physics: Conference Series, 733 012039, Published under licence by IOP Publishing Ltd. https://doi.org/10.1088/1742-6596/733/1/012039

[55] Patra, C. N. (2018). Solid lipid-based delivery system for oral delivery of drugs: A review. Asian Journal of Pharmaceutics (AJP), 12(04). https://doi.org/10.22377/ajp.v12i04.2902

[56] Torchilin, V. P. (2007). Micellar nanocarriers: pharmaceutical perspectives. Pharmaceutical research, 24, 1. https://doi.org/10.1007/s11095-006-9132-0

[57] Alkhamis, K. A., Allaboun, H., & Al-Momani, W. Y. (2003). Study of the solubilization of gliclazide by aqueous micellar solutions. Journal of Pharmaceutical Sciences 92(4), 839. https://doi.org/10.1002/jps.10350

[58] Osman, M., Høiland, H., & Holmsen, H. (1998). Micropolarity and microviscosity in the micelles of the heptapeptide biosurfactant “surfactin”. Colloids and Surfaces B: Biointerfaces, 11(4), 167. https://doi.org/10.1016/S0927-7765(98)00031-9

[59] Park, H., Lee, S. G., Kim, T. K., Han, S. J., & Yim, J. H. (2012). Selection of extraction solvent and temperature effect on stability of the algicidal agent prodigiosin. Biotechnology and Bioprocess Engineering, 17(6), 1232. https://doi.org/10.1007/s12257-012-0210-3

[60] Rastegari, B., Karbalaei-Heidari, H. R., Zeinali, S., & Sheardown, H. (2017). The enzyme-sensitive release of prodigiosin grafted β-cyclodextrin and chitosan magnetic nanoparticles as an anticancer drug delivery system: Synthesis, characterization and cytotoxicity studies. Colloids and Surfaces B: Biointerfaces, 158, 589. https://doi.org/10.1016/j.colsurfb.2017.07.044

[61] Fei, D., Liu, F.-F., Gang, H.-Z., Liu, J.-F., Yang, S.-Z., Ye, R.-Q., & Mu, B.-Z. (2020). A new member of the surfactin family produced by Bacillus subtilis with low toxicity on erythrocyte. Process Biochemistry, 94, 164. https://doi.org/10.1016/j.procbio.2020.04.022

[62] Dufour, S., Deleu, M., Nott, K., Wathelet, B., Thonart, P., & Paquot, M. (2005). Hemolytic activity of new linear surfactin analogs in relation to their physico-chemical properties. Biochim Biophys Acta, 1726(1), 87. https://doi.org/10.1016/j.bbagen.2005.06.015

[63] Liu, X., Wang, Z., You, Z., Wang, W., Wang, Y., Wu, W., Peng, Y., Zhang, S., Yun, Y., & Zhang, J. (2024). Transcriptomic analysis of cell envelope inhibition by prodigiosin in methicillin-resistant *Staphylococcus aureus*. Frontiers in Microbiology 15, 1333526. https://doi.org/10.3389/fmicb.2024.1333526

[64] El-Fouly, M. Z., Sharaf, A. M., Shahin, A. A. M., El-Bialy, H. A., & Omara, A. M. A. (2015). Biosynthesis of pyocyanin pigment by *Pseudomonas aeruginosa*. Journal of Radiation Research and Applied Sciences, 8(1), 36. https://doi.org/10.1016/j.jrras.2014.10.007

[65] Abdelaziz, A. A., Kamer, A. M. A., Al-Monofy, K. B., & Al-Madboly, L. A. (2023). *Pseudomonas aeruginosa*’s greenish-blue pigment pyocyanin: its production and

biological activities. Microbial Cell Factories, 22(1), 110. https://doi.org/10.1186/s12934-023-02122-1

[66] Yip, C.-H., Mahalingam, S., Wan, K.-L., & Nathan, S. (2021). Prodigiosin inhibits bacterial growth and virulence factors as a potential physiological response to interspecies competition. PLOS ONE, 16(6), e0253445. https://doi.org/10.1371/journal.pone.0253445

[67] Dai, X., Cheng, H., Bai, Z., & Li, J. (2017). Breast cancer cell line classification and its relevance with breast tumor subtyping [review]. Journal of Cancer, 8(16), 3131. https://doi.org/10.7150/jca.18457

[68] Soto-Cerrato, V., Llagostera, E., Montaner, B., Scheffer, G. L., & Perez-Tomas, R. (2004). Mitochondria-mediated apoptosis operating irrespective of multidrug resistance in breast cancer cells by the anticancer agent prodigiosin. Biochemical Pharmacology 68(7), 1345. https://doi.org/10.1016/j.bcp.2004.05.056

[69] Lins, J. C., ME, D. E. M., SC, D. O. N., & Adam, M. L. (2015). Differential genomic damage in different tumor lines induced by prodigiosin. Anticancer Research, 35(6), 3325. https://www.ncbi.nlm.nih.gov/pubmed/26026092

[70] Wang, Z., Li, B., Zhou, L., Yu, S., Su, Z., Song, J., Sun, Q., Sha, O., Wang, X., Jiang, W., Willert, K., Wei, L., Carson, D. A., & Lu, D. (2016). Prodigiosin inhibits Wnt/beta-catenin signaling and exerts anticancer activity in breast cancer cells. Proceedings of the National Academy of Sciences U S A, 113(46), 13150. https://doi.org/10.1073/pnas.1616336113

[71] Shi, F., Lu, L., Lv, P., Li, Y., Li, H., Chen, X., & Zhu, Y. (2020). Prodigiosin inhibits the proliferation and migration of mcf-7 breast cancer cells through the demethylation of mir-200c gene. Cancer Research, 80, 1755. https://doi.org/10.1158/1538-7445.AM2020-1755

[72] Akiyode, O., George, D., Getti, G., & Boateng, J. (2016). Systematic comparison of the functional physico-chemical characteristics and biocidal activity of microbial derived biosurfactants on blood-derived and breast cancer cells. Journal of Colloid and Interface Science, 479, 221. https://doi.org/10.1016/j.jcis.2016.06.051

[73] Cao, X. H., Liao, Z. Y., Wang, C. L., Cai, P., Yang, W. Y., Lu, M. F., & Huang, G. W. (2009). Purification and antitumour activity of a lipopeptide biosurfactant produced by Bacillus natto TK-1. Biotechnology and Applied Biochemistry, 52(Pt 2), 97. https://doi.org/10.1042/BA20070227

[74] Cao, X. H., Wang, A. H., Wang, C. L., Mao, D. Z., Lu, M. F., Cui, Y. Q., & Jiao, R. Z. (2010). Surfactin induces apoptosis in human breast cancer MCF-7 cells through a ROS/JNK-mediated mitochondrial/caspase pathway. Chemico-Biological Interactions, 183(3), 357. https://doi.org/10.1016/j.cbi.2009.11.027

[75] Duarte, C., Gudina, E. J., Lima, C. F., & Rodrigues, L. R. (2014). Effects of biosurfactants on the viability and proliferation of human breast cancer cells. AMB Express, 4, 40. https://doi.org/10.1186/s13568-014-0040-0

[76] Park, S. Y., Kim, J.-H., Lee, Y. J., Lee, S. J., & Kim, Y. (2013). Surfactin suppresses TPA-induced breast cancer cell invasion through the inhibition of MMP-9 expression. International Journal of Oncology, 42(1), 287. https://doi.org/10.3892/ijo.2012.1695

[77] Heerklotz, H., & Seelig, J. (2001). Detergent-like action of the antibiotic peptide surfactin on lipid membranes. Biophysical journal, 81(3), 1547. https://doi.org/10.1016/S0006-3495(01)75808-0

[78] Heerklotz, H., & Seelig, J. (2007). Leakage and lysis of lipid membranes induced by the lipopeptide surfactin. European Biophysics Journal, 36, 305. https://doi.org/10.1007/s00249-006-0091-5

[79] Wójtowicz, K., Czogalla, A., Trombik, T., & Łukaszewicz, M. (2021). Surfactin cyclic lipopeptides change the plasma membrane composition and lateral organization in mammalian cells. Biochimica et Biophysica Acta (BBA) - Biomembranes, 1863(12), 183730. https://doi.org/10.1016/j.bbamem.2021.183730